Estimation of the in-vivo minimum inhibitory concentration of cipargamin in uncomplicated *Plasmodium falciparum* malaria

Running title: Estimated MIC of cipargamin in malaria

Hien Tinh Tran,[a,d] *Nicholas J. White,*[b,d] *Thuy-Nhien Thanh Nguyen,*[a] *Hoa Thi Nhu,*[a] *Thuan Duc Phung,*[a] *Joel Tarning,*[b,d] *François Nosten,*[b,c,d] *Baldur Magnusson,*[e] *Jay Prakash Jain,*[f] *Kamal Hamed*[g#]

Oxford University Clinical Research Unit – Hospital for Tropical Diseases, Ho Chi Minh City, Vietnam[a]; Mahidol-Oxford Tropical Medicine Research Unit, Faculty of Tropical Medicine, Mahidol University, Bangkok, Thailand[b]; Shoklo Malaria Research Unit, Faculty of Tropical Medicine, Mahidol University, Mae Sot, Thailand[c]; Centre for Tropical Medicine and Global Health, Nuffield Department of Clinical Medicine, University of Oxford, Oxford, UK[d]; Novartis Pharma AG, Basel, Switzerland[e]; Novartis Healthcare Pvt. Ltd., Hyderabad, India[f]; Novartis Pharmaceuticals Corporation, East Hanover, NJ, USA[g]

Correspondence to:
Dr Kamal Hamed, Novartis Pharmaceuticals Corporation, One Health Plaza, East Hanover, NJ 07936, NJ, USA
kamal.hamed@novartis.com
Phone: +1 862 778 4780

Abstract

The minimum inhibitory concentration (MIC) of an antimalarial drug for a particular infection is the drug level associated with a net parasite multiplication rate of one per asexual cycle. To ensure cure of malaria the MIC must be exceeded until all parasites have been eliminated. The development of highly sensitive and accurate polymerase chain reaction quantitation of low-density malaria parasitemia enables prospective pharmacokinetic–pharmacodynamic (PK–PD) characterization of antimalarial drug effects, and now allows identification of the in-vivo MIC. An adaptive design and PK–PD modeling approach was used to determine prospectively the MIC of the new antimalarial cipargamin (KAE609) in adults with uncomplicated *Plasmodium falciparum* malaria, in an open-label, dose-ranging phase 2a study. Vietnamese adults with acute *P. falciparum* malaria were allocated sequentially to treatment with single 30 mg (n = 6), 20 mg (n = 5), 10 mg (n = 7), or 15 mg (n = 7) doses of cipargamin. Artemisinin-based combination therapy was given after parasite densities had fallen and then risen as cipargamin levels declined below the MIC, but before a return of signs or symptoms. The rates of parasite clearance were dose-dependent with near saturation of effect at an adult dose of 30 mg. The developed PK–PD model accurately predicted the therapeutic responses in 23/25 patients. The predicted median in-vivo MIC was 0.126 ng/mL (range 0.038–0.803 ng/mL). Pharmacometric characterization of the relationship between antimalarial drug concentrations and parasite clearance rates following graded sub-therapeutic antimalarial drug dosing is safe, and provides a rational framework for dose-finding in antimalarial drug development.

46 **Funding:** Novartis Pharma AG. TTH, NJW, NTTN, NTH, PDT, JT, and FN are
47 supported by the Wellcome Trust.

48 **Keywords:** malaria; resistance; cipargamin; pharmacokinetic–pharmacodynamic
49 model; clinical trial

INTRODUCTION

The emergence of resistance to current antimalarial drugs threatens to reverse recent substantial gains in the control and elimination of malaria. Several factors contribute to the emergence and spread of resistance, notably uncontrolled use of monotherapies, poor quality medicines, and systematic under-dosing (1, 2). Therefore, maximizing the lifetime of any new antimalarial drug depends not only on the propensity for resistance to arise or to share cross-resistance with existing drug classes but also on finding the best treatment dose during drug development (2).

An alternative to previous, largely empirical approaches to dose-finding for new antimalarial drugs is to determine prospectively, in vivo, the minimum inhibitory concentration (MIC) (2). The MIC has been defined as the plasma or blood concentration associated with a parasite multiplication rate of one per cycle, and therefore represents a therapeutic target that must be exceeded for a sufficient duration to guarantee cure (3). In recent years, ex-vivo experimental systems, animal models, and more recently, human challenge models have provided valuable information on antimalarial pharmacokinetic–pharmacodynamic (PK–PD) relationships, although their direct relevance to the treatment of symptomatic malaria remains uncertain (4). Ideally, the key PK–PD determinants of therapeutic response should be determined in the natural disease.

The spiroindolone cipargamin (formerly KAE609) is a new antimalarial drug with potent activity against *Plasmodium falciparum* and *Plasmodium vivax* (5–7). Cipargamin inhibits the P-type cation-translocating ATP-ase PfATP4, disturbing parasite sodium

72 homeostasis and causing osmotic dysregulation (5, 8, 9). This novel mechanism of
73 action affecting all stages of intraerythrocytic parasite development probably explains
74 why cipargamin treatment causes extremely rapid parasite clearance (5, 6, 10).

75 In the first study of its kind, we aimed to estimate prospectively the in-vivo MIC of
76 cipargamin in acute uncomplicated *P. falciparum* malaria. This was made possible by
77 the development of sensitive and accurate quantitative polymerase chain reaction
78 (qPCR) measurement of parasite nucleic acids, which permits tracking of parasitemia at
79 densities well below those causing illness, and thus, characterization of recrudescence
80 without discomfort or risk for the patient (11–13).

81

MATERIALS AND METHODS

Patients

Adult Vietnamese patients aged 20–60 years and weighing between 40 and 90 kg, with acute *P. falciparum* monoinfection confirmed by microscopy (asexual parasite count 5,000–50,000/μL), were recruited if they could take oral medications reliably and gave fully informed written consent to the study procedures, and if their axillary or oral/tympanic/rectal temperature was higher than ≥37.5°C or ≥38°C, respectively, at screening or during the previous 24 hours. Exclusion criteria included signs/symptoms of severe malaria, mixed *Plasmodium* infection, and use of an antimalarial drug within 2 months (see appendix).

Study design

An adaptive single-dose de-escalation design was employed. The study was performed at a single center in Vietnam in accordance with the ethical principles of the Declaration of Helsinki. The study protocol was approved by the ethics committee of the Vietnamese Ministry of Health, the Oxford Tropical Research Ethics Committee (OxTREC), and by the study center's institutional review board (ClinicalTrials.gov identifier: NCT01836458).

Six cipargamin dose evaluations with approximately eight patients per group, running in descending sequence (30, 20, 10, 5, 2, and 1 mg) until the MIC was identified, were planned, with the option of dose adjustment based on data arising during the study. The 30 mg adult dose has been shown previously to clear parasitemia (assessed by

microscopy) in less than 24 hours in both *P. falciparum and P. vivax* malaria (5). During and after each stratum the data monitoring committee decided whether to reduce, maintain, or increase the dose. Cipargamin capsules were supplied at doses of 1, 10, and 25 mg, and were administered orally as a single dose under direct observation (day 1).

In order to estimate the in-vivo MIC safely, it is necessary for parasitemia to fall below microscopy level of detection and then rise again as drug levels decline below the MIC. The antimalarial plasma concentration at the vertex of this approximate parabola is considered the MIC (2). Antimalarial treatment was given when there was an unequivocal rise in parasite densities indicating recrudescence, but before a return of signs or symptoms (see appendix). Thus, the national standard antimalarial treatment course of dihydroartemisinin-piperaquine (DHA-PPQ 40 mg/320 mg per tablet [Arterakine®]; four, two, and two tablets on days 1, 2, and 3, respectively) and primaquine (four 7.5 mg tablets as a single dose) was given to all patients on day 42, or earlier in the case of early treatment failure (ETF) or rising qPCR parasitemia. ETF was defined as clinical deterioration or lack of clinical/parasitemia improvement at 24 hours, parasitemia >75,000/μL at or after 12 hours post-dose, any parasitemia detected by microscopy with fever (≥48 hours post-dose), or parasitemia >100/μL based on microscopy without fever (≥72 hours post-dose).

Study assessments and procedures

Vital signs were recorded and blood samples taken every 4–6 hours until defervescence and two consecutive negative microscopy parasite counts, then once daily until day 8,

125 then on alternate days until day 28, and on days 35 and 42. Serial parasite densities
126 were measured from thick and thin blood film examinations at higher densities and then
127 by a validated real-time qPCR of the *P. falciparum* 18S rRNA gene (limit of detection: 22
128 parasites/mL) conducted in real time on site and reported daily to the clinical
129 investigators (14). Samples for ring-stage and gametocyte (Pfs25) mRNA transcripts
130 were also taken and measured at the Queensland Institute of Medical Research
131 Berghofer Medical Research Institute (15). Blood samples (3 mL) for plasma cipargamin
132 concentration measurements were taken at 0 (pre-dose), 0.5, 1, 2, 3, 4, 5, 6, 8, 10, 12,
133 16, 20, 24, 36, 48, 72, 96, 120, 144, and 168 hours after dosing. Samples were stored
134 at –70°C until analysis using a validated LC-MS/MS assay with a lower limit of
135 quantitation of 1 ng/mL (5, 10). More than 67% of the triplicate quality control samples
136 at five different concentrations were within ±15.0% of the individual values. Safety
137 assessments included monitoring of vital signs, laboratory values, urinalysis,
138 electrocardiogram, and adverse events (AEs) classified according to the Common
139 Terminology Criteria for Adverse Events (CTCAE, version 4.03)
140 (http://evs.nci.nih.gov/ftp1/CTCAE/CTCAE_4.03_2010-06-
141 14_QuickReference_5x7.pdf).

142 **In-vitro susceptibility testing**

143 The in-vitro susceptibility of *P. falciparum* to cipargamin was measured in pretreatment
144 blood samples using a 24-hour trophozoite maturation assay (16). Relative parasite
145 maturation and drug concentrations were fitted in GraphPad Prism v.6.01 (La Jolla,
146 California, USA) using the dose–response package. All response data were fitted

simultaneously to estimate the population mean slope of the dose–response curve and the IC_{50} value, and to characterize variability. All individual isolate data were fitted separately using the population slope estimate to generate robust estimates of the individual isolate IC_{50} values.

Assessments of parasite clearance

Parasite clearance metrics were assessed using the Worldwide Antimalarial Resistance Network parasite clearance estimator (17). Other efficacy endpoints are described in the appendix.

Pharmacokinetic modeling

Pharmacokinetics was described initially by non-compartmental analysis using Phoenix WinNonlin version 6.2 (Certara, Princeton, NJ, USA). PK–PD characteristics were then evaluated with nonlinear mixed-effects modeling in the software NONMEM v 7.3 (ICON Development Solutions, Ellicott City, MD, USA). The most appropriate model for pharmacokinetic (PK) characterization was developed by evaluating different absorption, disposition, and covariate models as well as random effects components (see appendix for details) (18, 19). Individual PK parameters from the final model were imputed into the PK–PD model to drive the cipargamin-dependent “parasite clearing” effect.

Pharmacodynamic modeling

166 Parasite densities (microscopy and qPCR) were transformed to total parasite burdens
167 assuming 80 mL whole blood/kg. In *P. falciparum* malaria, as asexual density declines,
168 gametocytemia rises, because mature gametocytes are released from sequestration
169 (20). DNA density estimates do not discriminate between asexual dividing, refractory,
170 and sexual parasites. To reduce confounding by gametocytemia, the qPCR DNA
171 density estimates were censored when sexual parasite densities (measured by Pfs25
172 mRNA) reached >10% of the total measurement (assuming a conservative estimate of
173 10 mRNA copies per cell in the Pfs25 assay). Recrudescent infections were identified
174 from rising qPCR DNA and confirmed by rising ring-stage mRNA together with
175 unchanged or falling Pfs25 transcript numbers; in some patients this was confirmed by
176 the appearance of asymptomatic microscopy-detectable asexual parasites. There was a
177 good correlation between uncensored PCR and microscopy measurements (data not
178 shown) and these data were therefore pooled for PK–PD modeling. Different structural
179 PK–PD models were evaluated to characterize the relationship between drug exposure
180 and parasite killing (see appendix). The MICs were taken directly from individually
181 predicted profiles in patients with recrudescence.

182 **Statistical analysis**

183 The projected sample size was based on operational rather than statistical
184 considerations (see appendix). Parasite clearance and fever clearance times were
185 analyzed using the Kaplan–Meier method (see appendix). The relationship between
186 cipargamin exposure, defined as observed area under the concentration–time curve
187 between 0 and 24 hours ($AUC_{0–24h}$) or as observed maximum concentration (C_{max}), and

parasite clearance half-life ($PC_{1/2}$) was modelled with a non-linear regression model (illustrated below for AUC_{0-24h}):

$PC_{1/2} = a + (b - a) \times e^{(-k \times AUC_{0-24h})}$ where a is the asymptotic maximal effect of cipargamin exposure on the $PC_{1/2}$, b is the longest $PC_{1/2}$ and k is the rate of decrease in $PC_{1/2}$.

RESULTS

Patients

Twenty-five adult Vietnamese male patients with acute uncomplicated falciparum malaria were enrolled between 15 January 2014 and 12 March 2015. The first three groups received cipargamin in descending dose order: 30 mg (*n* = 6), 20 mg (*n* = 5), and 10 mg (*n* = 7) (Table 1). One patient in the 30 mg group received 21 mg in error and was included in the 20 mg group for the analysis. Because of the inadequate therapeutic responses in the 10 mg group, dosing of the fourth group (*n* = 7) was increased to 15 mg. Sixteen patients received early rescue treatment (30 mg, *n* = 3/6; 20 mg, *n* = 2/5; 10 mg, *n* = 5/7; 15 mg, *n* = 6/7), four because of ETF and 12 because of later recrudescence (Fig. S1).

Therapeutic responses

Rates of fever and parasite clearance were approximately dose dependent (Table S1). Mean [SD] parasite clearance half-life ($PC_{1/2}$) estimates were 4.35 [2.21], 3.79 [1.22], 1.91 [1.64], and 1.47 [0.83] hours for 10, 15, 20, and 30 mg, respectively. An asymptotic non-linear model described the relationship between $PC_{1/2}$ and both $AUC_{0–24h}$ and C_{max} well and suggested saturation of the effect at higher doses of cipargamin (Fig. 1). Despite trends for increased 28-day PCR-corrected cure rate with higher doses and increased exposure (AUC) (Table S1), no individual PK parameter predicted cure (data not shown).

Safety

Nineteen (76%) patients reported at least one AE (Table S2). Three AEs in the 30 mg group were considered related to study treatment (nausea, myalgia, and headache). There were no serious AEs or AEs leading to study discontinuation. Most laboratory abnormalities did not exceed grade 2 severity; six patients had grade 3 abnormalities. One patient with a history of hypertension who received 30 mg had a rise in blood pressure to 160/100 mm Hg that resolved after treatment with furosemide 20 mg.

In-vitro susceptibility to cipargamin

Population estimates (95% CI) for slope and IC_{50} were -1.22 (-1.35 – -1.09) and 2.97 (2.70–3.26) ng/mL, respectively, with median (range; IQR) individual estimated IC_{50} values of 2.38 (0.468–17.2; 1.25–4.07) ng/mL.

Pharmacokinetic modeling

The PK properties of cipargamin were well described by a flexible transit-absorption model followed by a one-compartment disposition model (Fig. 2). Allowing inter-individual variability on the relative bioavailability significantly improved model fit. Body weight was incorporated as a fixed allometric function on clearance and volume parameters. Dose did not significantly affect the PK properties, suggesting dose-linear kinetics (Table 2, Table 3 and Fig. S2). The final PK model (Table 3) showed excellent overall diagnostic performance (Fig. S3 and S4).

Pharmacodynamic modeling

As individual-patient malaria-parasite multiplication rates (K_{GROW}) before drug administration are unknown, K_{GROW} was fixed to 10 per life-cycle (i.e. 48 hours) (21, 22). The initial implementation of the PK–PD model assumed a homogenous parasite population and first-order drug-dependent parasite removal (K_{KILL}). However, individual and population parasite clearance curves showed a clearly biphasic parasitemia decline that could not be explained adequately by gametocytemia. A small, refractory parasite subpopulation was considered the most likely explanation, and its incorporation significantly improved the model fit. The fraction of all asexual parasites that were refractory ($1\text{-}F_{SEN}$) was estimated but allowed for inter-individual variability. Their activation ("awakening"; K_{ACT}) and then removal was also estimated to explain cures. Higher doses and correspondingly higher plasma concentrations were associated with significantly faster maximum parasite killing rates (E_{MAX}). The final PK–PD model (Table 3) showed adequate overall diagnostic performance (Fig. S3 and S4) and characterized therapeutic responses correctly for 23 of the 25 patients (i.e. cure, ETF or later recrudescence; Fig. 3). The estimated median in-vivo MIC was 0.126 ng/mL (range 0.0375–0.803 ng/mL; IQR 0.0786–0.273 ng/mL), occurring at a median interval of 7.45 days (5.29–11.4 days; IQR 6.51–9.32 days) after drug administration for patients predicted correctly as having recrudescent infections (n = 12). Time to MIC is a function of dose as lower doses, and subsequently lower drug concentrations, will reach MIC values more rapidly than higher doses, assuming similar PK and parasite characteristics. Patients correctly predicted as cured (n = 7) showed a maximum median MIC value of 0.236 ng/mL (range 0.03–6.33 ng/mL; IQR 0.08–1.47 ng/mL), defined as the cipargamin concentration when predicted parasite numbers fell below 10.

DISCUSSION

Antimalarial drugs are deployed in combinations both to optimize efficacy and to prevent or delay the emergence of resistance (http://www.who.int/malaria/publications/atoz/9789241549127/en/). Fixed-dose combinations (FDCs) are needed to ensure adherence to both components and prevent use of monotherapies that could select individual drug resistance. It is essential that the optimum dose of a newly developed compound is chosen before the drug is tied in a FDC. While patients with partial immunity may clear partially treated infections, to ensure cure with the individual drug component in all patients, plasma concentrations must exceed the MIC for a sufficient time to eliminate all the blood stage parasites. Identifying the dose and dosing strategy that achieves this requires characterization of two independent variables: the population PK properties of the antimalarial drugs in the target populations, and the in-vivo drug susceptibility of infecting malaria parasite populations. The MIC can only be estimated accurately in vivo if there is recrudescence. As the MIC depends both on host factors, notably immunity, and the susceptibility of the infecting parasites, it is best assessed in patients from an area of low malaria transmission and consequently low background immunity where multidrug-resistant parasites are prevalent, such as in the present study. The final dosage in a combination regimen will be determined by the predicted duration for which the MIC is exceeded in all relevant patient groups (based on population PK modelling), global variations in malaria parasite susceptibility, practical considerations such as weight banding, any interactions with the partner drugs, and safety and tolerability (2). This first prospective determination of the in-vivo MIC in a dose-finding study was made possible by the

recent development of sensitive PCR quantitation methods. The MIC of cipargamin was determined safely without discomfort to the patients, all of whom received curative treatment before any signs or symptoms developed.

In this study the PK properties of the novel spiroindolone antimalarial, cipargamin, were described satisfactorily by a one-compartment disposition model with flexible absorption, and were similar to results from previous studies in malaria patients (5). Exposure to cipargamin was approximately dose proportional, as demonstrated previously in human volunteers (10). In the first exploratory studies conducted in Thai patients with *P. falciparum* or *P. vivax* malaria, cipargamin cleared parasitemia more rapidly than any other known antimalarial drug (5). In the current study, parasite clearance rates increased with increasing cipargamin exposure approaching a plateau with the 30 mg dose. The PK–PD modeling predicted MIC values ranging from 0.0375 to 0.803 ng/mL (median 0.126 ng/mL). In-vitro susceptibility was assessed by the trophozoite maturation test, which measures ring-stage susceptibility, the main determinant of parasite clearance. In the current study, conventional 48-hour in-vitro tests, which assess the full asexual cycle, mean IC_{50} values ranged from 0.195 to 0.546 ng/mL in laboratory isolates and were all below 3.9 ng/mL in fresh isolates from malaria patients. The results of this study suggest that the in-vivo MIC for cipargamin is in a concentration range associated with approximately 10% inhibition of trophozoite development and 20–50% inhibition of schizont maturation in ex-vivo systems (although the milieu and notably protein binding are different between the two).

In murine models, in which two compartment disposition models were fitted, cipargamin exposure (AUC) was a better determinant of parasite clearance than C_{max} after single doses (23). In this clinical study, a clear dose-response relationship was evident and a single compartment model fitted the concentration data satisfactorily. So, C_{max} and AUC were closely related and there was no clear superiority of one over the other as predictors of the parasitological response.

There are several limitations to PK–PD modeling based upon quantitative DNA estimates. First, DNA measurements do not distinguish between asexual and sexual stage parasites, nor between quiescent and dividing parasites. However, the drug effect being assessed is on dividing asexual stage parasites, and in the case of cipargamin reflects splenic clearance of red blood cells containing damaged, osmotically dysregulated parasites (24). As parasite densities decline, the more slowly cleared sexual stage parasites and any drug-refractory forms comprise an increasing proportion of the DNA signal. Recent ex-vivo studies suggest that cipargamin does not induce the same refractory forms observed with artemisinin drugs (25), so the nature of the parasite forms, which persist despite exposure to high cipargamin concentrations, clearly requires further study (25, 26). Low-dose primaquine was not given as a rapid gametocytocide in this study because cipargamin was considered to have gametocytocidal activity, but this was insufficient. Thus, in some cases, both as a result of drug-refractory parasite stages and persistent gametocytemia, the fall and subsequent rise in the observed DNA signal was “flat bottomed” rather than parabolic. Second, while ultrasensitive PCR is 1000 times more sensitive than microscopy, and can detect parasites down to densities of ~20/mL, parasite densities at MIC were

sometimes lower than this detection threshold; in both cases the MIC had to be extrapolated rather than observed. Detection of mRNA is potentially more sensitive than detection of DNA as there are potentially thousands of mRNA transcripts per cell, but their numbers vary with time, making accurate parasite quantitation potentially difficult. However, changing values are very useful as indicators of trend, and so informed the DNA-based assessments. For example, rising parasite DNA at a time of rising numbers of ring-stage mRNA transcripts and falling gametocyte mRNA unequivocally identified parasite multiplication.

In conclusion, the rates of *P. falciparum* parasite clearance were dose dependent, with near saturation of the maximum effect at a cipargamin dose of 30 mg. The PK–PD model developed accurately predicted the therapeutic responses in the majority of falciparum malaria patients.

CONTRIBUTORS

NJW, BM, JPJ, and KH were involved in protocol design. TTH, NTTN, NTH, and PDT were involved in data collection. TTH, NJW, JT, FN, BM, JPJ, and KH were involved in data analysis. Each author reviewed and/or edited drafts of the manuscript, and each author approved the final submitted version.

ACKNOWLEDGMENTS

The authors thank Ruobing Li and Fan Yang for providing clinical operational support for this study, Micha Levi for supporting the PK–PD modeling, and James McCarthy of QIMR Berghofer Medical Research Institute, Brisbane, Queensland, Australia for providing advice and analytic services for the Pfs25 and ring-stage assays, funded by Novartis Pharma AG. This study was part of the Wellcome Trust Tropical Medicine Research Programs in Vietnam and Thailand and was supported by Novartis Pharma AG. Medical writing support was provided by Magdy Fahmy, PhD, at Seren Communications, and was funded by Novartis Pharma AG.

FUNDING INFORMATION

The sponsor was involved in study design and in data collection, analysis, and interpretation. All authors had full access to the data and are responsible for their accuracy and completeness. The corresponding author had final responsibility for the decision to submit this report for publication.

DECLARATION OF INTERESTS

TTH, NJW, NTTN, NTH, PDT, JT and FN have no conflicts of interest to declare. BM is an employee of Novartis Pharma AG, Basel, Switzerland. JPJ is an employee of Novartis Healthcare Private, Ltd., Hyderabad, India. KH is an employee of Novartis Pharmaceuticals Corporation, East Hanover, New Jersey, USA.

References

1. **Barnes KI, Watkins WM, White NJ.** 2008. Antimalarial dosing regimens and drug resistance. Trends Parasitol **24:**127–134.
2. **White NJ.** 2013. Pharmacokinetic and pharmacodynamic considerations in antimalarial dose optimization. Antimicrob Agents Chemother **57:**5792–5807.
3. **White NJ.** 1997. Assessment of the pharmacodynamic properties of the antimalarial drugs in-vivo. Antimicrob Agents Chemother **41:**1413–1422.
4. **Craig AG, Grau GE, Janse C, Kazura JW, Milner D, Barnwell JW, Turner G, Langhorne J.** 2012. The role of animal models for research on severe malaria. PLoS Pathogens **8:**e1002401.
5. **White NJ, Pukrittayakamee S, Phyo AP, Rueangweerayut R, Nosten F, Jittamala P, Jeeyapant A, Jain JP, Lefèvre G, Li R, Magnusson B, Diagana TT, Leong FJ.** 2014. Spiroindolone KAE609 for falciparum and vivax malaria. N Engl J Med **371:**403–410.
6. **Rottmann M, McNamara C, Yeung BK, Lee MC, Zou B, Russell B, Seitz P, Plouffe DM, Dharia NV, Tan J, Cohen SB, Spencer KR, González-Páez GE, Lakshminarayana SB, Goh A, Suwanarusk R, Jegla T, Schmitt EK, Beck HP, Brun R, Nosten F, Renia L, Dartois V, Keller TH, Fidock DA, Winzeler EA, Diagana TT.** 2010. Spiroindolones, a potent compound class for the treatment of malaria. Science **329:**1175–1180.
7. **Diagana TT.** 2015. Supporting malaria elimination with 21st century antimalarial agent drug discovery. Drug Discov Today **20:**1265–1270.

8. **Spillman NJ, Kirk K.** 2015. The malaria parasite cation ATPase PfATP4 and its role in the mechanism of action of a new arsenal of antimalarial drugs. Int J Parasitol Drugs Drug Resist **5:**149–162.

9. **Spillman NJ, Allen RJ, McNamara CW, Yeung BK, Winzeler EA, Diagana TT, Kirk K.** 2013. Na(+) regulation in the malaria parasite Plasmodium falciparum involves the cation ATPase PfATP4 and is a target of the spiroindolone antimalarials. Cell Host Microbe **13:**227–237.

10. **Leong FJ, Li R, Jain JP, Lefèvre G, Magnusson B, Diagana TT, Pertel P.** 2014. A first-in-human randomized, double-blind, placebo-controlled, single- and multiple-ascending oral dose study of novel antimalarial Spiroindolone KAE609 (Cipargamin) to assess its safety, tolerability, and pharmacokinetics in healthy adult volunteers. Antimicrob Agents Chemother **58:**6209–6214.

11. **McCarthy JS, Sekuloski S, Griffin PM, Elliott S, Douglas N, Peatey C, Rockett R, O'Rourke P, Marquart L, Hermsen C, Duparc S, Möhrle J, Trenholme KR, Humberstone AJ.** 2011. A pilot randomised trial of induced blood-stage Plasmodium falciparum infections in healthy volunteers for testing efficacy of new antimalarial drugs. PLoS One **6:**e21914.

12. **Kamau E, Tolbert LS, Kortepeter L, Pratt M, Nyakoe N, Muringo L, Ogutu B, Waitumbi JN, Ockenhouse CF.** 2011. Development of a highly sensitive genus-specific quantitative reverse transcriptase real-time PCR assay for detection and quantitation of plasmodium by amplifying RNA and DNA of the 18S rRNA genes. J Clin Microbiol **49:**2946–2953.

13. **Andrews L, Andersen RF, Webster D, Dunachie S, Walther RM, Bejon P, Hunt-Cooke A, Bergson G, Sanderson F, Hill AV, Gilbert SC.** 2005. Quantitative real-time polymerase chain reaction for malaria diagnosis and its use in malaria vaccine clinical trials. Am J Trop Med Hyg **73:**191–198.

14. **Imwong M, Hanchana S, Malleret B, Rénia L, Day NP, Dondorp A, Nosten F, Snounou G, White NJ.** 2014. High-throughput ultrasensitive molecular techniques for quantifying low-density malaria parasitemias. J Clin Microbiol **52:**3303–3309.

15. **Pasay CJ, Rockett R, Sekuloski S, Griffin P, Marquart L, Peatey C, Wang CY, O'Rourke P, Elliott S, Baker M, Möhrle JJ, McCarthy JS.** 2016. Piperaquine monotherapy of drug-susceptible Plasmodium falciparum infection results in rapid clearance of parasitemia but is followed by the appearance of gametocytemia. J Infect Dis **214:**105–113.

16. **Chotivanich K, Tripura R, Das D, Yi P, Day NP, Pukrittayakamee S, Chuor CM, Socheat D, Dondorp AM, White NJ.** 2014. Laboratory detection of artemisinin-resistant Plasmodium falciparum. Antimicrob Agents Chemother **58:**3157–3161.

17. **Flegg JA, Guerin PJ, White NJ, Stepniewska K.** 2011. Standardizing the measurement of parasite clearance in falciparum malaria: the parasite clearance estimator. Malar J **10:**339.

18. **Savic RM, Jonker DM, Kerbusch T, Karlsson MO.** 2007. Implementation of a transit compartment model for describing drug absorption in pharmacokinetic studies. J Pharmacokinet Pharmacodyn **34:**711–726.

19. **Holford NH.** 1996. A size standard for pharmacokinetics. Clin Pharmacokinet **30:**329–332.

20. **Thomson D.** 1911. A research into the production, life and death of crescents in malignant tertian malaria in treated and untreated cases, by an enumerative method. Ann Trop Med Parasitol **5:**57–82.

21. **Simpson JA, Aarons L, Collins WE, Jeffery GM, White NJ.** 2002. Population dynamics of untreated Plasmodium falciparum malaria within the adult human host during the expansion phase of the infection. Parasitology **124**(Pt 3)**:**247–63.

22. **Dietz K, Raddatz G, Molineaux L.** 2006. Mathematical model of the first wave of Plasmodium falciparum asexual parasitemia in non-immune and vaccinated individuals. Am J Trop Med Hyg **75**(Suppl 2)**:**46–55.

23. **Lakshminarayana SB, Freymond C, Fischli C, Yu J, Weber S, Goh A, Yeung BK, Ho PC, Dartois V, Diagana TT, Rottmann M, Blasco F.** 2015. Pharmacokinetic-pharmacodynamic analysis of spiroindolone analogs and KAE609 in a murine malaria model. Antimicrob Agents Chemother **59:**1200–1210.

24. **Zhang R, Suwanarusk R, Malleret B, Cooke BM, Nosten F, Lau YL, Dao M, Lim CT, Renia L, Tan KS, Russell B.** 2016. A basis for rapid clearance of circulating ring-stage malaria parasites by the spiroindolone KAE609. J Infect Dis **213:**100–104.

25. **Chavchich M, Van Breda K, Rowcliffe K, Diagana TT, Edstein MD.** 2016. The spiroindolone KAE609 does not induce dormant ring stages in Plasmodium falciparum parasites. Antimicrob Agents Chemother **60:**5167–5174.

454 26. **Huskey SE, Zhu CQ, Fredenhagen A, Kühnöl J, Luneau A, Jian Z, Yang Z,**
455 **Miao Z, Yang F, Jain JP, Sunkara G, Mangold JB, Stein DS.** 2016. KAE609
456 (cipargamin), a new spiroindolone agent for the treatment of malaria: evaluation
457 of the absorption, distribution, metabolism, and excretion of a single oral 300-mg
458 dose of [14C]KAE609 in healthy male subjects. Drug Metab Dispos **44:**672–682.

459 **Tables and figures**

460

461 **TABLE 1** Patient demographics and baseline characteristics by cipargamin dose

	Dose 1: 30 mg (*n* = 6)	**Dose 2: 20 mg (*n* = 5[a])**	**Dose 3: 10 mg (*n* = 7)**	**Dose 4: 15 mg (*n* = 7)**	**Total (*n* = 25)**
Age, years					
Mean (SD)	33.2 (12.91)	32.2 (6.98)	30.6 (8.24)	34.7 (8.79)	32.7 (9.04)
Median (range)	33.5 (20–52)	30.0 (23–41)	30.0 (20–42)	35.0 (20–46)	31.0 (20–52)
Sex					
Male, *n* (%)	6 (100)	5 (100)	7 (100)	7 (100)	25 (100)
Predominant race					
Asian, *n* (%)	6 (100)	5 (100)	7 (100)	7 (100)	25 (100)
Height, cm					
Mean (SD)	168.8 (5.49)	163.8 (5.36)	163.7 (8.30)	161.9 (2.41)	164.4 (6.06)
Median (range)	167.5 (163–176)	162.0 (157–171)	162.0 (150–175)	161.0 (159–165)	164.0 (150–176)
Weight, kg					

Mean (SD)	60.7 (7.45)	56.8 (3.35)	60.8 (11.41)	56.9 (5.44)	58.9 (7.56)
Median (range)	63.5 (50–69)	57.0 (53–62)	60.0 (42–78)	59.0 (50–65)	59.0 (42–78)
Body mass index, kg/m^2					
Mean (SD)	21.3 (2.65)	21.2 (1.16)	22.5 (2.42)	21.7 (2.07)	21.7 (2.12)
Median (range)	20.8 (18.8–25.7)	21.0 (20.2–23.1)	22.9 (18.7–26.4)	23.0 (18.6–23.9)	21.2 (18.6–26.4)

462 [a] One patient in the 30 mg cohort received 21 mg in error (a 1 mg capsule was
463 mistakenly administered in place of the required 10 mg capsule). This patient was
464 analyzed with the 20 mg cohort for all analyses.
465 SD, standard deviation.
466

467 **TABLE 2** Summary of individual pharmacokinetic parameter estimates from the final
468 model describing cipargamin pharmacokinetics in patients with uncomplicated
469 *P. falciparum* malaria

Parameter[a]	Dose 30 mg (*n* = 6)	Dose 20 mg (*n* = 5)	Dose 15 mg (*n* = 7)	Dose 10 mg (*n* = 7)
C_{max} (ng/mL)	597 (248–687)	535 (434–678)	442 (312–618)	247 (155–413)
T_{max} (h)	3.51 (2–10)	3.00 (2–4)	3.00 (2–4)	4.02 (2–6)
AUC_{inf} (µg.h/mL)	16.7 (7.75–18.80)	10.1 (8.30–15.60)	11.3 (5.28–14.40)	6.4 (3.87–9.10)
$T_{1/2}$ (h)	16.7 (12.2–29.2)	15.4 (12.0–16.2)	14.9 (11.4–28.8)	17.3 (15.6–25.0)

470 All values are reported as median (range).

471 C_{max}, maximum (peak) plasma drug concentration after drug administration; T_{max}, time
472 to reach C_{max}; AUC_{inf}, accumulated area under the plasma concentration–time curve
473 from time zero to infinity; $T_{1/2}$, terminal elimination half-life.

474 [a] Individual post-hoc empirical Bayes estimates from the final population
475 pharmacokinetic model.

476

477 **TABLE 3** Population parameter estimates of the final model describing cipargamin
478 pharmacokinetics and pharmacodynamics in patients with uncomplicated *P. falciparum*
479 malaria

Parameter	Population estimate[a] (% RSE[b])	95% CI[b]	% CV for IIV[a] (% RSE[b])	95% CI[b]
Pharmacokinetic model				
CL/F (L/h)	1.72 (5.69)	1.55–1.94	18.5 (12.4)	13.5–21.8
V/F (L)	40.6 (4.71)	37.3 –44.7	–	–
Nr. trans comp	3 *fix*	–	–	–
MTT (h)	0.867 (12.6)	0.682–1.11	65.2 (13.5)	47.5–79.9
Ka (h^{-1})	1.65 (25.2)	1.04–2.81	176 (30.4)	107–312
F (%)	100 *fix*	–	26.2 (25.3)	13.6–37.6
σ (% CV)	17.5 (10.3)	14.3–21.1	–	–
Pharmacodynamic model				
K_{GROW} (h^{-1})	0.0479 *fix*	–	–	–
E_{MAX} (h^{-1})	0.564 (12.9)	0.383–0.710	62.2 (33.6)	45.1–90.2
EC_{50} (ng/mL)	0.354 (16.7)	0.222–0.466	–	–
F_{SEN} (%)	99.1 (0.132)	98.8–99.4	81.8 (39.2)	58.9–194
K_{ACT} (h^{-1})	0.0987 (14.7)	0.0592–0.123	41.5 (42.0)	30.2–67.7
COV_{Dose_Emax}	0.0463 (14.9)	0.0318–0.0604	–	–
σ (%)	109 (17.0)	94.8–178	–	–

CL/F, apparent elimination clearance; V/F, apparent volume of distribution; Nr. trans comp, number of transit compartments in the absorption model; MTT, mean transit time through the transit compartments; Ka, first-order absorption rate constant from the last transit compartment to the central compartment; F, relative oral bioavailability; σ, unexplained residual error. K_{GROW}, parasite multiplication rate, fixed to 10-fold multiplication per 48-hour cycle; E_{MAX}, maximum effect (maximum parasite reduction rate); EC_{50}, concentration needed for 50% of maximum effect; F_{SEN}, fraction of total asexual parasites which were fully drug sensitive; K_{ACT}, first-order rate constant for refractory parasites to become active; COV_{Dose_Emax}, exponent of the relationship between dose and E_{MAX} (i.e. $\theta_i = \theta_{TVEmax} \times (Dose/10)^{\wedge}COV_{Dose\_Emax}$).

[a] Population mean values and inter-individual variability (IIV) were estimated by NONMEM. Coefficient of variation (% CV) for IIV was calculated as $100 \times \sqrt{e^{\text{estimate}} - 1}$. Population mean parameter estimates were calculated for a typical patient with a body weight of 59 kg receiving a study drug dose of 10 mg.

[b] Relative standard error (RSE) was calculated as 100 × (standard deviation/mean parameter estimate) from 1,000 and 500 successful iterations for the PK and PK–PD models, respectively, of a nonparametric bootstrap diagnostic. The 95% confidence interval (95% CI) was characterized as the 2.5 to 97.5 percentiles of the bootstrap estimates.

502 **FIG 1** A) Parasite clearance half-life vs $AUC_{0–24h}$ and B) parasite clearance half-life vs

503 C_{max}

504

505 Circles represent individual AUCs, the color represents the corresponding cipargamin

506 dose, and the blue line and shaded area represents LOESS smooth with the uncertainty

507 band. [a] From study X2201; [b]From study X2202. $AUC_{0–24h}$, area under the plasma

508 concentration–time curve during from time zero to 24 hours post-dose.

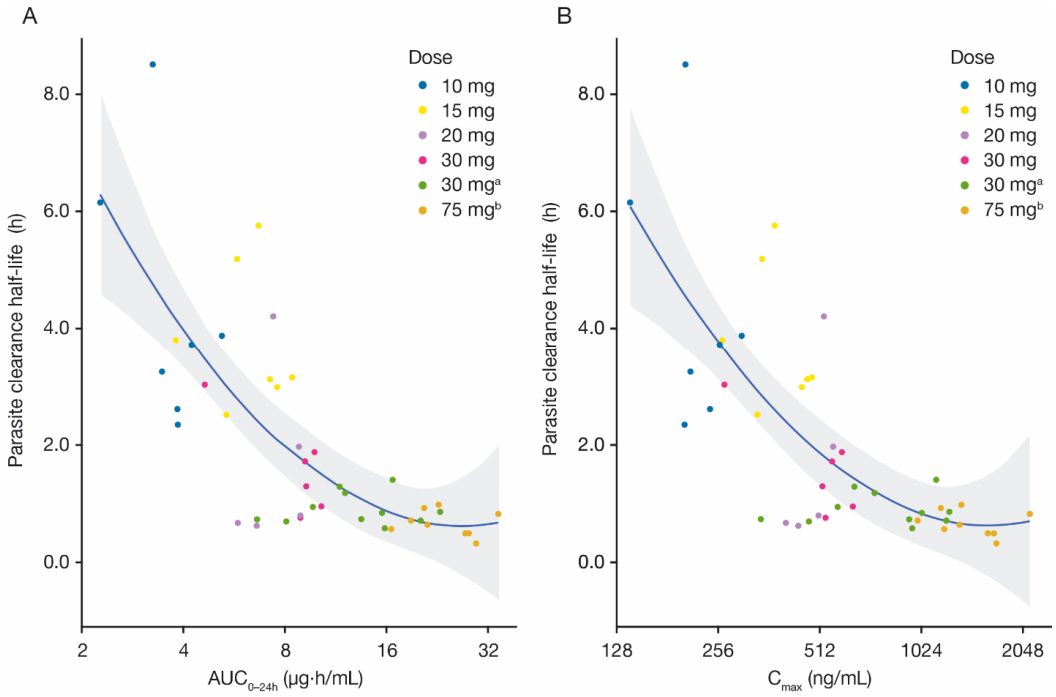

509

FIG 2 Schematic representation the final model describing cipargamin pharmacokinetics and pharmacodynamics in patients with uncomplicated *P. falciparum* malaria

The fraction of asexual parasites that were fully drug sensitive was estimated at enrollment, and the observed total parasitemia is the sum of sensitive and refractory parasites.

CL/V, apparent elimination clearance; C_p, cipargamin plasma concentration; EC_{50}, concentration needed for 50% of maximum effect; E_{MAX}, maximum effect (maximum parasite reduction rate; dose-dependent as specified in Table 3); F, relative oral bioavailability; Ka, first-order absorption rate constant from the last transit compartment to the central compartment; K_{ACT}, first-order rate constant for refractory parasites to become active; K_{GROW}, parasite multiplication rate, fixed to 10-fold multiplication per 48-hour cycle; K_{KILL}, first-order rate constant for cipargamin-dependent parasite kill; KTR, first-order transit rate constant; MTT, mean transit time through the transit compartments; V/F, apparent volume of distribution.

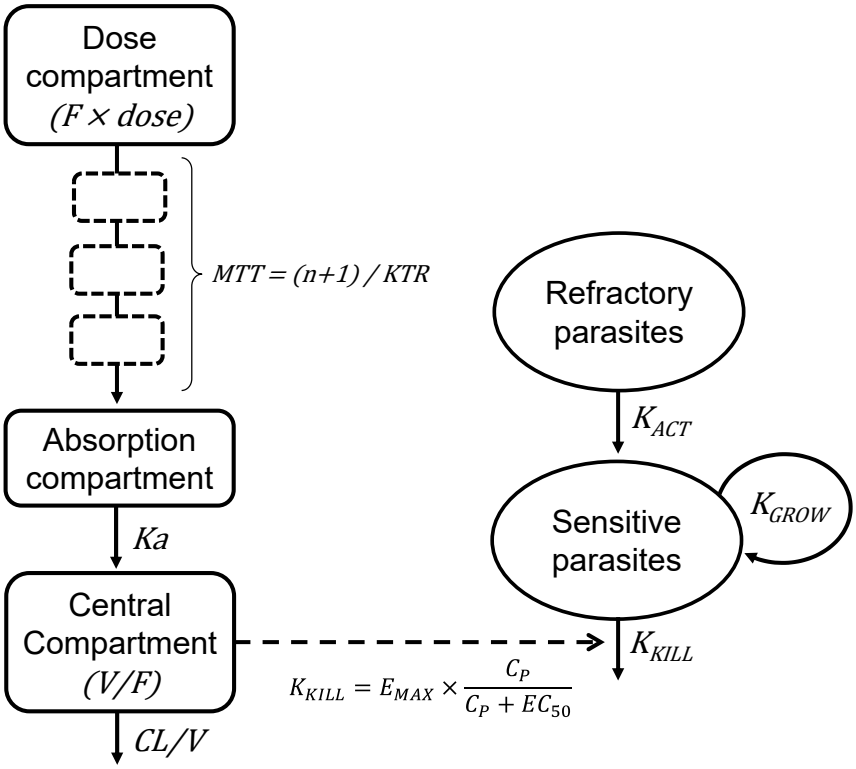

524

525

526 **FIG 3** Individually predicted parasite clearance curves, using the final model describing
527 cipargamin pharmacokinetics and pharmacodynamics in patients with uncomplicated
528 *P. falciparum* malaria

529

530 Each solid line represents predicted total parasite load after dosing over time for an
531 individual patient. The broken horizontal lines indicate the level of microscopy detection.

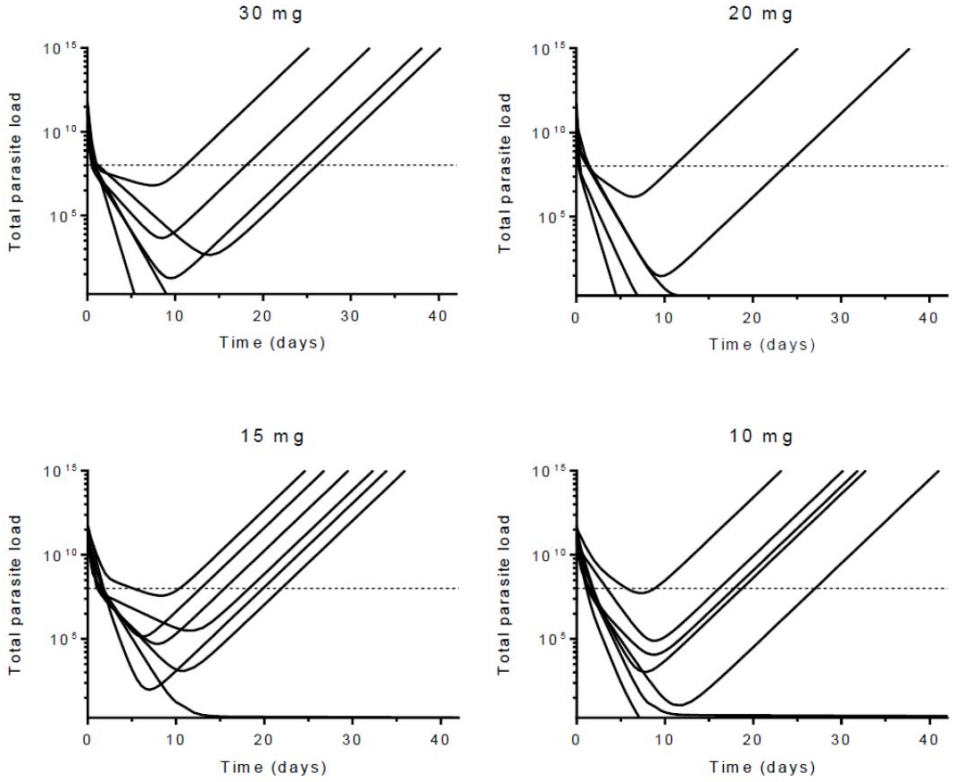

532